

# A 6.25 Mbps, 12.4 pJ/bit DQPSK Backscatter Wireless Uplink for the NeuroDisc Brain-Computer Interface

James Rosenthal, *Student Member, IEEE*, <sup>‡</sup>Eleftherios Kampionakis, *Student Member, IEEE*,  
<sup>‡</sup>Apoorva Sharma, *Student Member, IEEE*, and Matthew S. Reynolds, *Senior Member, IEEE*

**Abstract**—Wireless brain-computer interfaces (BCIs) used for fundamental neuroscience research in freely moving non-human primates (NHPs) require communication systems capable of transferring large volumes of recorded neural data while consuming minimal power. We introduce a 6.25 Mbps differential quadrature phase-shift keying (DQPSK) backscatter wireless uplink for the NeuroDisc BCI, operating in the 902-928 MHz industrial, scientific, and medical (ISM)-band. The backscatter uplink consumes 77.5  $\mu\text{W}$  (only 0.06% of the system power budget), yielding a communication energy efficiency of 12.4 pJ/bit, while the measured error vector magnitude of the DQPSK constellation is 9.69%. The neural recording front-end has a measured input-referred noise of 2.35  $\mu\text{V}_{\text{rms}}$  at a maximum sampling rate of 20 kSps. We present end-to-end recording and wireless uplink validation with pre-recorded neural data as well as *in vivo* recordings from a pigtail macaque.

**Index Terms**—implanted biomedical devices, neural recording, backscatter communication

## I. INTRODUCTION

Brain-computer interface (BCI) applications include both neuroscience research and clinical development. In research, BCIs are used on a broad range of subject animals, including rats [1], [2] and non-human primates (NHPs) [3]–[5], to understand neurophysiological behavior by recording electrophysiological signals and, in the case of bi-directional BCIs, to stimulate neurons or ensembles with electrical current or light (optogenetic stimulation).

Fundamental neuroscience research continues to be the driver for increasingly capable BCIs with increased channel count and more capable on-board processing. At the same time, the goals of reduced size, weight, and power consumption (SWAP) result in significant engineering challenges, particularly where untethered freely behaving animals are involved and battery life is a major experimental constraint.

Conventional wireless data links such as Bluetooth Low Energy (BLE), IEEE 802.11 (WiFi) were not designed for the high data rate and low power consumption requirements of

The project described was supported in part by Award Number EEC-1028725 from the National Science Foundation. The content is solely the responsibility of the authors and does not necessarily represent the official views of the National Science Foundation.

<sup>‡</sup>A. Sharma and <sup>‡</sup>E. Kampionakis contributed equally to this work.

J. Rosenthal, E. Kampionakis, and A. Sharma are with the Department of Electrical Engineering, University of Washington, Seattle, WA 98195, USA.

M. S. Reynolds is with the Department of Electrical Engineering and the Paul G. Allen School of Computer Science and Engineering, University of Washington.

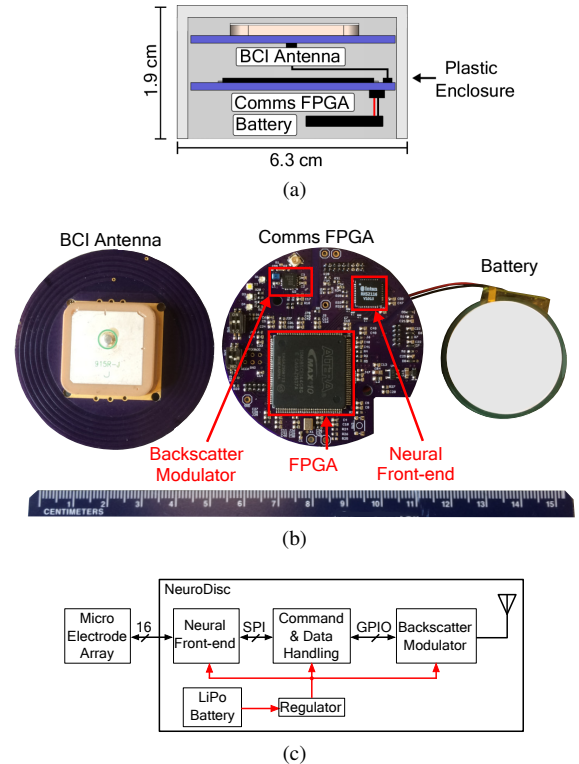


Fig. 1: (a) NeuroDisc mechanical stackup (b) Photo of the NeuroDisc sub-assemblies (c) Block diagram of the Comms FPGA board

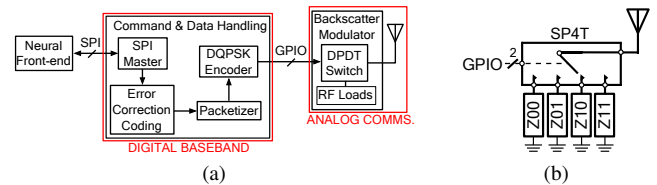


Fig. 2: (a) Comms FPGA data flow detail (b) DQPSK backscatter modulator detail

multi-channel wireless BCIs. As an alternative to conventional radios for BCI uplinks, backscatter uplinks offer the potential for high data rates with ultra low power consumption in a small form factor, with far better energy efficiency than existing semi-custom active radios (e.g. [2], [3], [5]).

Backscatter communication moves the analog power and complexity burden of carrier generation and amplification out

of the BCI itself into a more power-rich external device. Thus, backscatter uplinks offer reduced SWAP, and allow for longer battery life, as shown in Table I. Prior BCI devices using backscatter communication [1] use amplitude shift keying (ASK) or load modulation to achieve backscatter communication with a spectral efficiency of 1 bit per symbol, over a short range of  $<15$  mm. In contrast, the NeuroDisc uses differential quadrature phase shift keying (DQPSK) which encodes 2 bits per symbol and provides 6.25 Mbps of data throughput while consuming only  $78 \mu\text{W}$  in the backscatter modulator, yielding an uplink energy efficiency of 12.4 pJ/bit. The *in vivo* measurements presented here were taken at a communication distance of 0.3 m, while further *in vitro* measurements demonstrated a reliable backscatter uplink inside a 93 cm x 93 cm x 77 cm (height x width x length) NHP home cage [6].

## II. NEURODISC SYSTEM OVERVIEW

The NeuroDisc is a wireless bi-directional brain-computer interface (BBCI) designed for electrophysiology experiments in non-human primates. The NeuroDisc provides a low-power 16-channel bidirectional electrophysiology interface that can sample neural signals at rates up to 20 kSps, enabling measurements of both local field potentials and neural spikes. The system is composed of the three parts shown in Fig. 1: the Comms FPGA board, a semi-custom antenna [6], and a 3.7 V 500 mAh single-cell lithium polymer battery providing  $\sim 12$  hours of operation. The NeuroDisc wirelessly interfaces to a custom full-duplex UHF backscatter receiver which is used to receive, record, and analyze data packets in real time. It is differentiated from other BCI devices by its high-rate DQPSK backscatter data uplink that consumes only 0.06% of the total power budget (Table I).

### A. Comms FPGA Board

As shown in the block diagram of Fig. 2a, the Comms FPGA board provides the core functionality of the NeuroDisc. An Intan RHS2116 biosignal front-end IC enables both recording and stimulation. The RHS2116 requires a single-supply +3.3 V rail for recording, or a dual-supply of up to  $\pm 9$  V for stimulation. It includes a high-gain AC and low-gain DC amplifier stage with 16-bit and 10-bit analog-to-digital converters for each channel, respectively.

The command-and-data-handling block leverages an Altera MAX10 FPGA running from a 50 MHz clock to manage the SPI interface with the neural front-end, receive digitized neural samples, packetize the data, and stream DQPSK-modulated symbols to the backscatter modulator. The MAX10 includes non-volatile configuration flash memory which reduces the system size. The RHS2116 IC outputs 32-bits of payload data at each sample. The FPGA encodes this payload data using a Hamming (16, 11) error correcting code (ECC) to allow for single bit-error correction and dual bit-error detection at the receiver. The 16-bit words of encoded data are then assembled into a packet totaling 64 words (1024 bits) that includes 16-bit synchronization frame markers and a packet counter (Fig. 3). In total, each packet contains 416 bits of sampled biological

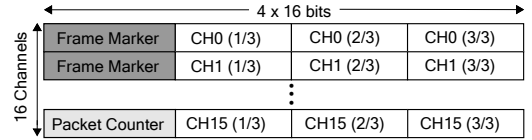


Fig. 3: Packet structure - each packet is 1024 bits long, containing 416 bits of biosignal data prior to ECC

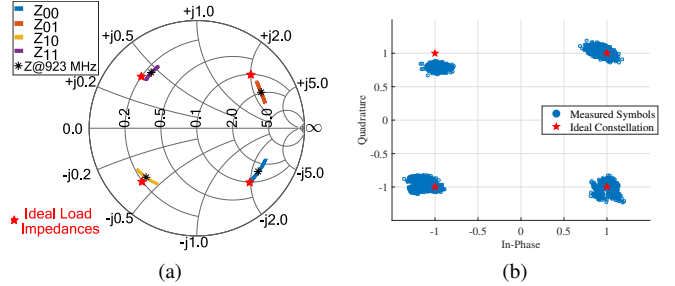


Fig. 4: (a) Impedance measurements of the DQPSK backscatter modulator states across the 900 MHz ISM band (b) Recorded symbol constellation over 5,000 symbol periods with a calculated EVM of 9.69% (adapted from [6])

data: 16 bits per channel from the AC high-gain amplifier and 10 bits per channel from the DC high-gain amplifier.

Packets are mapped into two-bit DQPSK symbols and fed to a backscatter modulator implemented with an Analog Devices ADG904 SP4T RF switch with four pre-determined impedances at its terminals. The ideal values for these impedances were calculated using the method of [7], and we selected the closest commercially-available components; the small deviation of the measured constellation points from the ideal ones is due to the slight difference in component values, component tolerances, and the parasitic impedances of the ADG904. Fig. 4 presents the measured impedances across the North American UHF ISM band frequencies (902-928 MHz). The reflection coefficients for the four different switch states form a constellation on the Smith Chart that corresponds to the four symbol states of the DQPSK backscatter signal.

### B. BCI Antenna

The BCI antenna shown in Fig. 1 is a 55 mm diameter, two-layer PCB using 1.6 mm-thick FR-4 substrate. On the top side, an Abracon APAE915R2540ABDB1-T ceramic patch antenna is bonded to a circular ground plane with a 15 mm radius. The 10 dB return loss bandwidth was measured to extend from 921.5 to 928 MHz, providing a 6.5 MHz bandwidth.

### C. External-System Backscatter Uplink Receiver

The external system receiver was designed around the Ettus USRP B210 software-defined radio (SDR). The receiver is configured for a full-duplex monostatic backscatter communication architecture, and includes a custom full-duplex self-jammer cancellation system, and a software back-end implemented in GNUradio and Matlab.

The USRP generates a continuous wave carrier at 923 MHz which is then backscatter modulated by the NeuroDisc. The

TABLE I: Comparison of state-of-the-art wireless BCIs

	<i>Borton et al., 2013 [4]</i>	<i>Miranda et al., 2010 [3]</i>	<i>Schwarz et al., 2014 [5]</i>	<i>Szuts et al., 2011 [2]</i>	<i>Muller et al., 2015 [1]</i>	<i>This Work</i>
<b>Test Subject</b>	NHP	NHP	NHP	Rat	Rat	<b>NHP</b>
<b>BCI Size (mm)</b>	56 x 42 x 11	38 x 38 x 51	- <sup>a</sup>	60 x 30 x 30	6.4 x 6.4 x 0.7	<b>63 x 63 x 19</b>
<b>Recording &amp; Stimulation</b>	<b>X</b>	<b>X</b>	<b>X</b>	<b>X</b>	<b>X</b>	<b>✓</b>
<b>ADC (bits)</b>	12	12	12	- <sup>a</sup>	15	<b>16</b>
<b>No. of Channels</b>	8	32	512	64	64	<b>4 Ch. @ 20 kSps, 16 Ch. @ 5 kSps</b>
<b>Sampling (kSps)</b>	20	30	31.25	20	1	<b>5 - 20</b>
<b>RF Comms Type</b>	Active RF	Active RF	Active RF	Active RF	ASK Backscatter	<b>DQPSK Backscatter</b>
<b>RF Comms Band</b>	3.8 GHz	3.7 - 4.1 GHz	2.4 GHz	2.4 GHz	300 MHz	<b>923 MHz</b>
<b>Wireless Data Rate (Mbps)</b>	24	24	1.33	12	1	<b>6.25</b>
<b>Uplink Distance (m)</b>	1	>20	- <sup>a</sup>	60	0.013	<b>0.3<sup>c</sup></b>
<b>Analog Comms Power (mW)</b>	≥30 <sup>a</sup>	30	33.9 <sup>b</sup>	200	0.0024	<b>0.078<sup>d</sup></b>
<b>Analog Comms Energy Efficiency (pJ/bit)</b>	≥1,250 <sup>a</sup>	1,250	25,488	16,000	2.4	<b>12.4</b>

<sup>a</sup>Exact value not reported. <sup>b</sup>TX power consumption of the nRF24L01+ at 0 dBm transmit power.

<sup>c</sup>Free-space distance for *in vivo* measurements. <sup>d</sup>Measured static+dynamic power.

TABLE II: Selection of DQPSK modulator impedances

<b>Z</b>	Ideal Impedance States		Actual Impedance States
	L/C Value	$\Gamma$	L/C
$Z_{00}$	1.74 pF	0.5 - j0.5	1.5 pF
$Z_{01}$	17.39 nH	0.5 + j0.5	20 nH
$Z_{10}$	8.7 pF	-0.5 - j0.5	8.4 pF
$Z_{11}$	3.48 nH	-0.5 + j0.5	3.3 nH

USRП receives the backscattered signal, downconverts it to I/Q baseband, and samples the baseband signal at up to 50 MSps. These sampled I/Q symbols are sent to a desktop PC that supports near-real time packet processing. The external system antenna is a Laird Technologies S9028PCR right-hand circularly polarized, air dielectric patch antenna with a 10 dB return loss bandwidth of 902-928 MHz. The reported antenna gain is 8 dBic with a 70° beamwidth, and its overall dimensions are 25.8 cm x 25.8 cm x 3.2 cm (length x width x height). Since freely moving animals may have any pose relative to the receiver antenna, a circularly polarized antenna can reduce signal losses from polarization mismatch.

### III. DQPSK BACKSCATTER MODULATOR DESIGN

Load impedances can be selected to implement arbitrary  $M$ -ary QAM backscatter constellations, as shown in [7]. To implement  $M$ -ary backscatter modulation,  $M$  load impedances,  $Z_1 \dots Z_M$ , are needed to represent the  $M$  different symbols in the constellation. These load impedances can be determined by first specifying the desired reflection coefficients,  $\Gamma_1 \dots \Gamma_M$ , for each modulation state. We start by specifying the  $i$ -th ideal modulation state in the constellation by its in-phase and quadrature components,  $(I_i, Q_i)$ , where  $|I_i| \leq 1$  and  $|Q_i| \leq 1$ . The complex reflection coefficients are:

$$\Gamma_i = I_i + jQ_i. \quad (1)$$

The load impedance for the  $i$ -th modulation state can be calculated by:

$$Z_i = -Z_a \frac{\alpha\Gamma_i + 1}{\alpha\Gamma_i - 1}, \quad (2)$$

where  $\alpha$  is a scaling constant between 0 and 1. As  $\alpha$  approaches 1, the backscatter system reflects increasing amounts of incident RF power, thus increasing the backscatter signal strength. For this work,  $\alpha$  was chosen to be  $\frac{1}{\sqrt{2}}$ , which yielded the ideal impedance values shown in Table II. Actual impedance values differ due to component variations and parasitic impedances.

## IV. EXPERIMENTAL RESULTS

### A. Laboratory Characterization and Validation

The NeuroDisc was first characterized in a benchtop setup using a Faraday cage to reduce 60 Hz pick-up, with a cabled RF system to uplink the data. To characterize the backscatter modulator, we measured the error vector magnitude (EVM) of the backscatter constellation as well as the energy efficiency of the backscatter modulator. The EVM is a key figure of merit for how well the measured constellation performs relative to the ideal DQPSK constellation [8]:

$$\text{EVM} = 100 \cdot \sqrt{\frac{\frac{1}{N} \sum_{k=1}^N |\hat{S}_{k_{ideal}} - S_{k_{sample}}|^2}{\frac{1}{N} \sum_{k=1}^N |\hat{S}_{k_{ideal}}|}}, \quad (3)$$

where  $N$  is the total number of symbols transmitted,  $S_{k_{sample}}$  is the normalized  $k$ -th demodulated symbol location in the I/Q plane, and  $\hat{S}_{k_{ideal}}$  is the ideal normalized symbol position. The measured EVM is 9.69 %, and the measured constellation is shown in Fig. 4(b).

To measure the modulator energy consumption, the ADG904 RF switch was supplied with +3.3 V by a Keithley source-meter, and an Agilent 33500B Waveform Generator drove the switch at a symbol rate of 3.125 M DQPSK

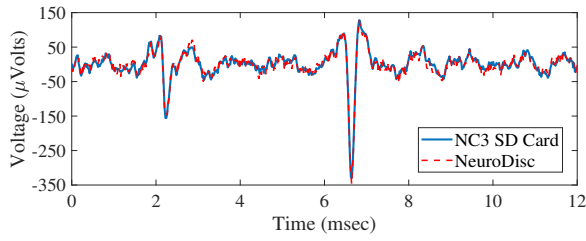


Fig. 5: Plot of pre-recorded neural spike data recorded by the reference BCI (NeuroChip3) and the NeuroDisc. Good agreement can be seen between the two systems.

symbols/s for a bit rate of 6.25 Mbps. The measured current was  $23.5 \mu\text{A}$ , yielding a DC power consumption of  $77.5 \mu\text{W}$ .

Input-referenced neural amplifier noise with the entire system running was measured by grounding all sixteen neural channels. The measured input-referenced noise was  $2.35 \mu\text{Vrms}$ , which shows good agreement with the  $2.4 \mu\text{Vrms}$  noise specified in the RHS2116 datasheet. As a final benchtop validation, pre-recorded neural signals containing local field potential (LFP) and spike data was fed into the NeuroDisc board, as well as a reference BCI system (University of Washington NeuroChip3, a new iteration of the NeuroChip2 [9]) from an Agilent 33500B arbitrary waveform generator. For the reference BCI (NC3), recorded data was saved to its on-board SD card, while for the NeuroDisc, recorded data was wirelessly uplinked to the external systems. Both BCIs were configured to sample at 5 kHz with a 1 Hz - 2 kHz band-pass filter as well as a 1.6 Hz DSP high-pass filter. As shown in Fig 5, good agreement can be seen between the NeuroDisc recording and the overlaid NeuroChip3 reference recording.

### B. In Vivo Recordings

*In vivo* recordings on an anesthetized pigtail macaque (*Macaca nemestrina*) were made to validate the performance of the NeuroDisc biosignal front-end and wireless backscatter uplink. The experiments were conducted at the Washington National Primate Research Center, Seattle, Washington, USA, with the support of the UW Department of Physiology and Biophysics, and all experimental procedures were approved by the UW Institutional Animal Care and Use Committee.

The NeuroDisc was connected via 17 cm of shielded single-ended cabling to a chronically-implanted 96-channel Utah Array (Blackrock Microsystems), previously implanted in the primary motor cortex (M1). The monkey rested on a plastic surgical cart, and the NeuroDisc was placed horizontally at the edge of the cart so that the BCI antenna had a clear line-of-sight to an external system antenna placed 30 cm away (Fig. 6). For this experiment, the NeuroDisc was configured to sample eight channels at 5 kHz with a 1 Hz - 2 kHz band-pass filter as well as a 1.6 Hz DSP high-pass filter. Sampled data was then uplinked at 6.25 Mbps to the external system, where it was decoded and plotted, as shown in Fig. 7.

### V. CONCLUSIONS AND FUTURE WORK

We introduce a 6.25 Mbps DQPSK backscatter uplink for the NeuroDisc BCI. The system has a measured input-referred

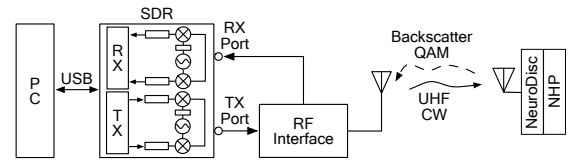


Fig. 6: Test setup for *in vivo* recordings with an NHP.

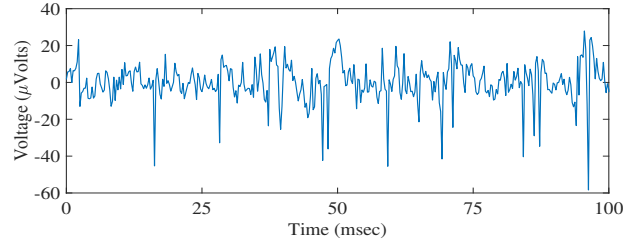


Fig. 7: Example of wirelessly uplinked *in vivo* neural spike recordings from the primary motor cortex of a pigtail macaque.

noise of  $2.35 \mu\text{Vrms}$ , a communication energy efficiency of 12.4 pJ/bit, and a DQPSK constellation EVM of 9.69%. The wireless uplink and BCI neural front-end were successfully validated by using pre-recorded data and *in vivo* recordings from a pigtailed macaque. Future work includes reducing noise in neural recordings by shortening cables to the neural front-end and exploring new antenna designs to improve the available bandwidth. Lastly, the analog communication efficiency could be improved by reducing the supply voltage to the RF switch, using an FPGA with lower static power, and/or developing a custom integrated circuit with an inductor-free DQPSK modulator using the approach of [7].

### ACKNOWLEDGMENT

The authors would like to thank Eberhard E. Fetz, Steve I. Perlmuter, Larry Shupe, Richy Yun, Andrew Bogaard, and the team at the Washington National Primate Research Center for their assistance and support.

### REFERENCES

- [1] R. Muller *et al.*, "A minimally invasive 64-channel wireless  $\mu\text{ECoG}$  implant," *IEEE J. Solid-State Circuits*, vol. 50, no. 1, pp. 344–359, 2015.
- [2] T. A. Szuts *et al.*, "A wireless multi-channel neural amplifier for freely moving animals," *Nature Neuroscience*, vol. 14, no. 2, p. 263, 2011.
- [3] H. Miranda *et al.*, "HermesD: A high-rate long-range wireless transmission system for simultaneous multichannel neural recording applications," *IEEE Trans. Biomed. Circuits Syst.*, vol. 4, no. 3, pp. 181–191, June 2010.
- [4] D. A. Borton *et al.*, "An implantable wireless neural interface for recording cortical circuit dynamics in moving primates," *Journal of Neural Engineering*, vol. 10, no. 2, p. 026010, 2013.
- [5] D. A. Schwarz *et al.*, "Chronic, wireless recordings of large-scale brain activity in freely moving rhesus monkeys," *Nature Methods*, vol. 11, no. 6, p. 670, 2014.
- [6] A. Sharma, E. Kampianakis *et al.*, "Wideband UHF DQPSK backscatter communication in reverberant cavity animal cage environments," *IEEE Trans. on Antennas and Propagation (TAP) (in revision)*, 2018.
- [7] S. J. Thomas *et al.*, "Quadrature amplitude modulated backscatter in passive and semipassive UHF RFID systems," *IEEE Trans. on Microwave Theory and Techniques*, vol. 60, no. 4, pp. 1175–1182, April 2012.
- [8] S. Thomas and M. S. Reynolds, "QAM Backscatter for Passive UHF RFID Tags," in *Proc. 2010 IEEE Intl. Conf. RFID (RFID 10)*, April 2010, pp. 210–214.
- [9] S. Zanos *et al.*, "The Neurochip-2: an autonomous head-fixed computer for recording and stimulating in freely behaving monkeys," *IEEE Trans. Neural Syst. Rehabil. Eng.*, vol. 19, no. 4, pp. 427–435, 2011.